Design of an interlocked four-port MIMO antenna for UWB automotive communications

CrossMark

M. Saravanan[1] (iD), R. Kalidoss[2], B. Partibane[2] and K. S. Vishvaksenan[2]

[1]Department of Electronics and Communication Engineering, Anand Institute of Higher Technology, Kazhipattur, Chennai 603 103, India and [2]Department of Electronics and Communication Engineering, Sri Sivasubramaniya Nadar College of Engineering, Kalavakkam, Chennai 603 110, India

CAMBRIDGE
UNIVERSITY PRESS

Abstract

The design, analysis, fabrication, and testing of a four-port multiple-input multiple-output (MIMO) antenna is reported in this paper for automotive communications. The MIMO antenna is constructed using the basic antenna element exploiting a slot geometry. Two such antennas are developed on the same microwave laminate to develop a two-port MIMO antenna. Two such microwave laminates are interlocked to create the four-port MIMO scheme. The most distinct feature of the proposed architecture is that the inter-port isolation is well-taken care without the need for an external decoupling unit. The four-port MIMO antenna has an overall volume of $32 \times 15 \times 32 \text{ mm}^3$. The prototype MIMO antenna is fabricated and the measurements are carried out to validate the simulation results. The antenna offers ultra-wideband (UWB) characteristics covering the frequency range of 2.8–9.5 GHz. The average boresight gain of the antenna ranges from 3.2 to 5.41 dBi with the peak gain at 8 GHz. The simulated efficiency of the antenna is greater than 73% within the operating bandwidth. The MIMO parameters such as envelope correlation coefficient, diversity gain, and mean effective gain are evaluated and presented. The appropriateness of the proposed antenna for deployment in the shark fin housing of the present-day automobiles is verified using on-car performance estimation.

Introduction

Automotive communications have received tremendous research interest in the recent past. The present-day automobiles are equipped with a plurality of information and entertainment services. These services are aimed to improve the travel experience of both the driver and the passengers. With an increase in the number of services, the antenna requirement also increases. Furthermore, the automotive scenario is complex due to the changing environment and hence changing channel conditions. Establishing a reliable communication link is a real challenge and addressing this issue is of paramount importance. To tackle this issue, present-day automobiles exploit the use of two diverse technologies, viz. ultra-wideband (UWB) and multiple-input multiple-output (MIMO) communications. The UWB systems are characterized by bandwidth greater than 500 MHz in which the information is spread. On the other hand, MIMO communication uses multiple antennas to transmit and receive information signals. The integration of UWB with MIMO reaps most of the benefits in a rich scattering environment. This paper is devoted to the development of a novel UWB MIMO antenna for use in automotive communications. Though the size of the car is huge, there are only notable locations where the antennas can be loaded for satisfactory performance. Car's roof is an ideal place to locate antennas since it is free from obstruction and is far above the ground eliminating the ground reflections. Thus the development of antennas that can be loaded into the shark fin housing of the automobiles receives considerable research interest. In the literature, several research works are reported on the development of planar MIMO antennas covering the UWB spectrum. These MIMO antennas are typically characterized by two ports or four ports. Since the channel capacity increases with the number of ports, this paper focuses on the development of a four-port MIMO antenna.

The monopole antennas are a wise choice for the development of UWB and MIMO antennas due to their attractive features such as wide bandwidth, compact size, and good radiation efficiency. In [1], a UWB two-element MIMO antenna with the isolated ground is presented using circular monopole and a quarter loop radiating elements. A two-element MIMO antenna with a reflector to enhance the isolation is reported in [2]. A structure shared UWB MIMO antenna with monopole and Vivaldi characteristics is reported in [3]. The antenna in [3] offers gain greater than 2.6 dBi and the envelope correlation coefficient (ECC) is very close to zero. A frequency-agile MIMO antenna with four-port UWB characteristics is reported in [4]. The antenna in [4] offers a 101% impedance bandwidth. A compact UWB antenna with fence type isolation enhancement structure is reported in [5] for MIMO
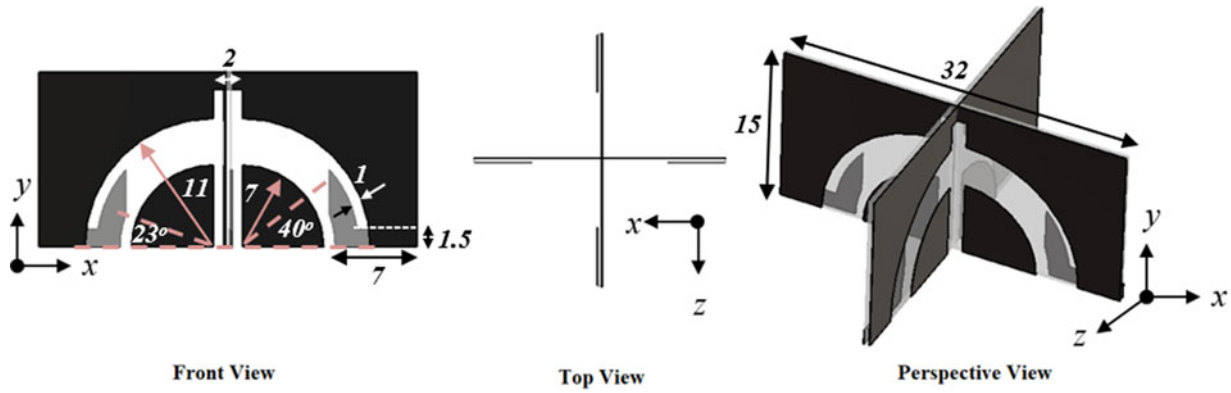
Fig. 1. The different views of the proposed four-port interlocked MIMO antenna (all the units are in mm).
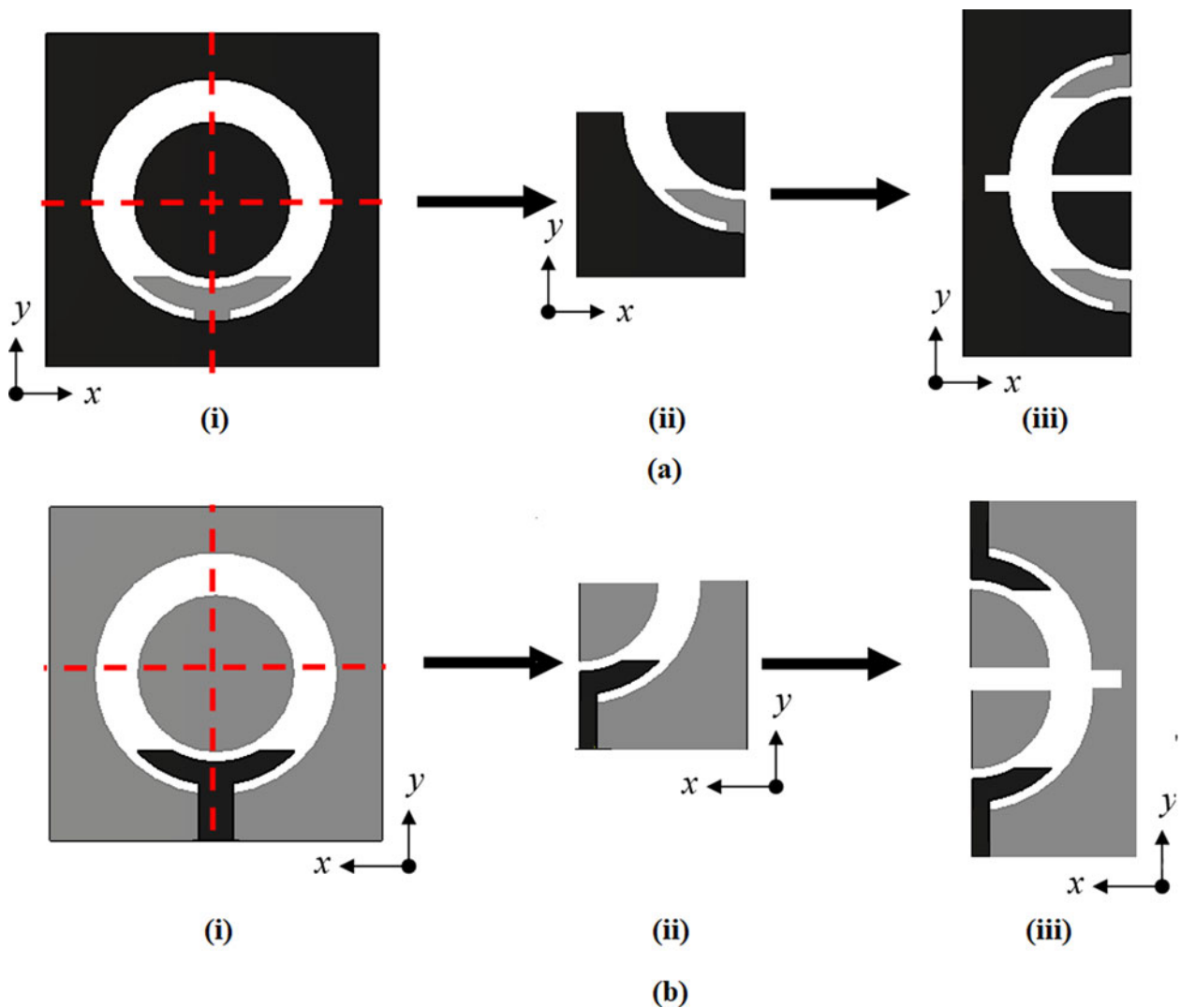

Fig. 2. Evolution of the proposed antenna element (i) Reference antenna, (ii) Proposed slot antenna, (iii) Two-port MIMO antenna developed on a single microwave laminate, (a) Front view, (b) Rear view (black: top metal; gray: bottom metal).

communications. A four-port two-element MIMO antenna operating from 2.7 to 3.6 GHz is reported in [6] for 5G applications in portable devices. The authors in [7] report the design of a two-element and a four-element MIMO antenna covering 3.6–

10.6 GHz. A hexagonal-shaped coplanar waveguide (CPW) fed UWB antenna is reported in [8]. A compact UWB MIMO antenna with dual-band elimination characteristics is reported in [8]. However, all these antennas in [7–9] are designed with
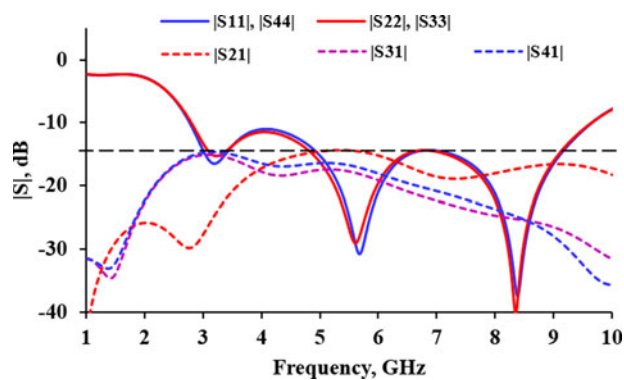
Fig. 3. Simulated *S*-parameter characteristics of the proposed four-port MIMO antenna.

Fig. 5. Measured *S*-parameter characteristics of the proposed four-port MIMO antenna.
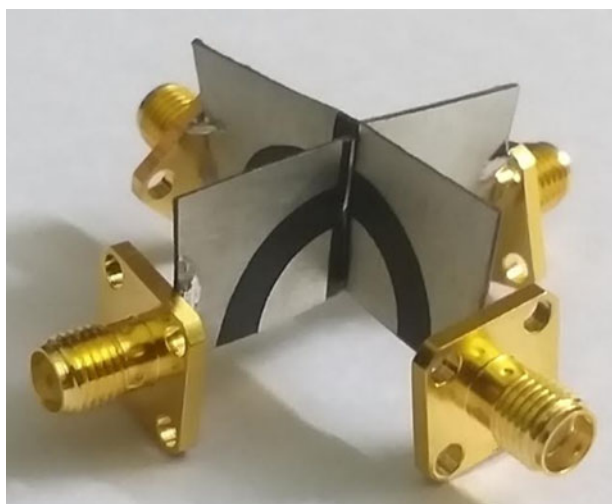

Fig. 4. Photograph of the fabricated prototype.

isolated ground structures. A novel double-sided UWB MIMO antenna is reported in [10]. The MIMO antenna in [10] offers isolation greater than 20 dB using electromagnetic bandgap structures. A multiband four-port MIMO antenna with complementary split-ring resonators (CSRR) for isolation enhancement is reported in [11]. Many other MIMO antennas [12–15] are reported in the literature for smartphone applications. Thus from the study of the literature, the need for the development of MIMO antennas that suits the requirements in automobiles is still a hot topic in antenna research. Some of the three-dimensional (3D) antennas are presented in [16–18]. A complicated 3D design is adopted in [17, 18]. These 3D antennas are also limited by the fact they have isolated ground structures.

Thus, this paper reports a four-port vertically polarized MIMO antenna covering the frequencies from 2.8 to 9.5 GHz. The antenna is designed on a low loss Taconic substrate and offers high mounting flexibility. In addition to the evaluation of the MIMO metrics, the prototype antenna is simulated in the presence of the vehicle's body and the results are presented. This paper is organized as follows. Section "MIMO antenna design & simulation" elaborates the design of the four-port MIMO antenna. The fabrication and measurements are discussed as described in the section "Fabrication and measurement". The section "Performance evaluation of MIMO metrics" presents the
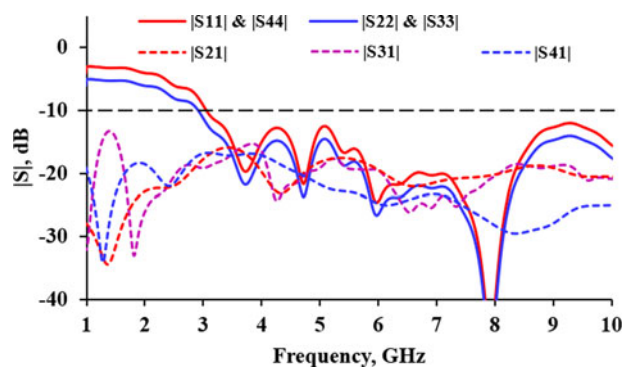
MIMO performance evaluation and the section "On-car performance evaluation" presents the on-car performance of the proposed four-port MIMO antenna, and finally, the conclusion is presented in the last section.

MIMO antenna design and simulation

The geometry of the proposed slot-based four-port MIMO antenna is shown in Fig. 1. The antenna is constructed using a low loss of 0.5 mm thin Taconic TLX9 substrate with dielectric constant 2.5 and loss tangent 0.0015. The array consists of two interlocked printed circuit boards (PCBs) where each PCB consists of two slot radiators as shown in Fig. 1(a). The top view and the perspective view of the interlocked MIMO scheme are shown in Figs 1(b) and 1(c), respectively. The basic antenna element in the PCB consists of one-quarter sector corresponding to the annular slot ring antenna.

The evolution of the basic antenna element is described in Fig. 2. The reference antenna is an annular ring antenna which exhibits structural symmetry along the *x*-axis. The antenna is excited by a microstrip line terminated by a sector-shaped stub line of sector length defined by two arc angles 23° and 40°, respectively. The annular ring is defined by an inner and outer radius of 7 and 11 mm, respectively. This proposed slot antenna is constructed from one bottom quadrant of the annular ring antenna in Fig. 2(a). The bisected slot antenna is shown in Fig. 2(b). The antenna in Fig. 2(b) is replicated through mirror imaging to create the two-port MIMO antenna as illustrated in Fig. 2(c). The antennas are separated by a distance of 2 mm. To have a connected ground configuration, the top metal of both the slot antennas is connected by a simple microstrip line of length 2 mm and width 1 mm. The footprint of the proposed two-element antenna in Fig. 2(c) is $32 \times 15 \text{ mm}^2$. The two-port MIMO antenna is extended to four-port by creating a slit in the substrate and adopting the interlocking scheme as shown in Fig. 1(c). The interlocking scheme results in the generation of vertically polarized signals making the antenna suitable for roof top-loading under the shark fin housing. The optimized size o the proposed antenna is $32 \times 15 \times 32 \text{ mm}^3$. The antenna design and simulations are carried out using CST Microwave Studio. The reflection coefficient characteristics and the mutual coupling characteristics of the proposed four-port MIMO antenna are shown in Fig. 3. During the design, port 1 and port 3 are connected to the antennas sharing the same PCB while port 2 and port 4 are connected to the antennas printed on the orthogonal
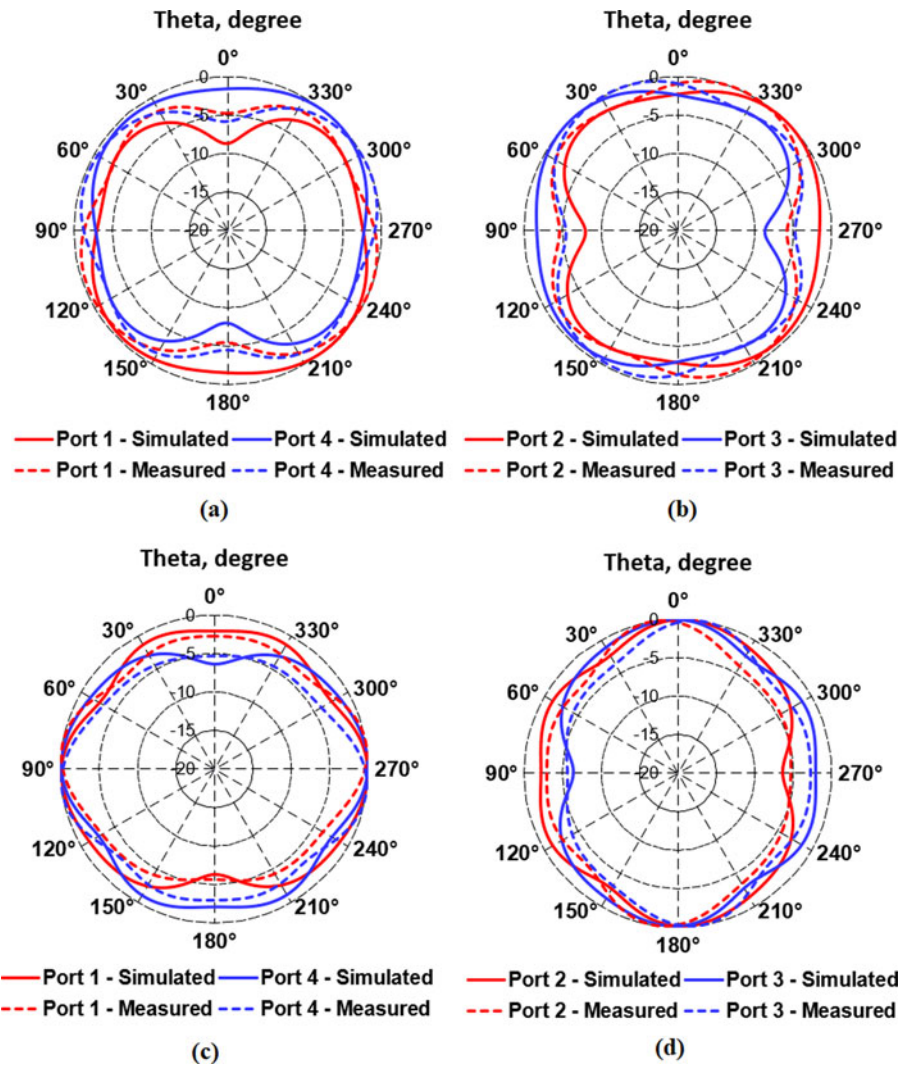
Fig. 6. Measured radiation pattern at 6 GHz (a and b) and 8 GHz (c and d).

PCB. Thus, the characteristics calculated from port 1 are identical to port 4 and the characteristics calculated from port 2 are identical to port 3. From the figure, it is evident that the proposed MIMO antenna offers UWB characteristics covering frequencies from 2.8 to 9.5 GHz with a reference voltage standing wave ratio (VSWR) of 2 corresponding to $|S_{11}| \leq -10$ dB. The antenna ports are separated by a large distance and hence the proposed antenna offers inherently high isolation. The calculated isolation is greater than 15 dB throughout the operational bandwidth. Thus, the proposed configuration does not require a separate decoupling arrangement to enhance the isolation characteristics of the MIMO antenna. The arrangement of the antennas is done in such a way that, the Port 1(2) and Port 3(4) offer polarization diversity while all the ports offer different radiation patterns with pattern maxima at different directions resulting in pattern diversity. Thus, the proposed configuration contributes to both polarization and pattern diversity.

Fabrication & measurement

S-parameter characteristics

The prototype MIMO antenna is fabricated using photolithography and the fabricated prototype is shown in Fig. 4. A total

of 50 Ω sub-miniaturized A (SMA) connectors are used to connect the feedlines of the proposed MIMO antenna. The antenna S-parameter measurements are carried out using Keysight's microwave analyzer N9917A. The measured S-parameter characteristics are shown in Fig. 5. The measured S-parameters are in close correlation with the simulation results. The measured reflection coefficient bandwidth starts from 2.95 GHz and extends over 10 GHz. However, the radiation pattern is not stable for frequencies over 10 GHz. Thus, the fundamental operating limit is considered to be 9.5 GHz as calculated in simulation. The measured port-to-port isolation with reference to port 1 to other ports is greater than 15 dB. The difference between the simulated and measured reflection coefficient is attributed to the fabrication tolerance and loss due to SMA soldering. The real-time interlocking has resulted in small air gaps which are also attributed to the deviation.

Radiation characteristics

The radiation characteristics of the proposed four-port MIMO antenna is shown in Fig. 6 for the two reference frequencies, viz. 6 and 8 GHz. The simulated radiation characteristics provide an average peak gain of the antenna is 5.41 dBi at 8 GHz with an efficiency greater than 73%. The radiation characteristics are
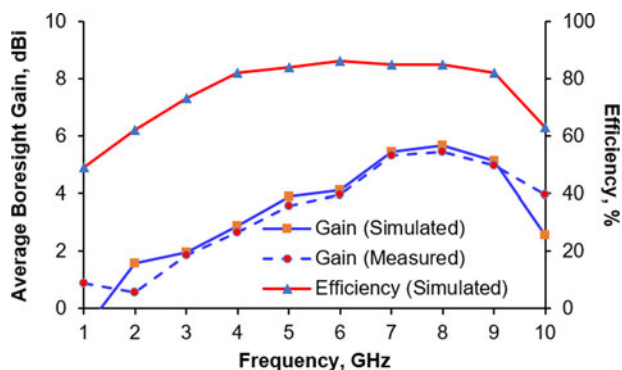
Fig. 7. Gain and efficiency characteristics of the proposed four-port MIMO antenna.

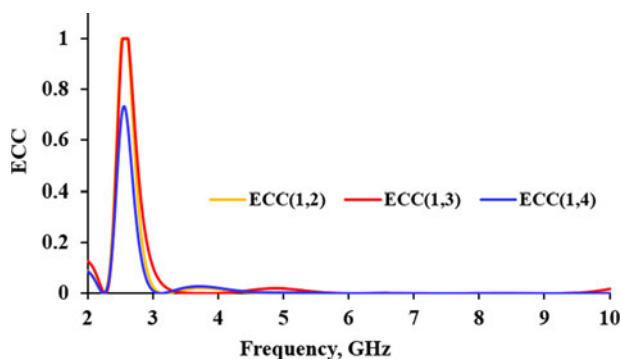**Fig. 9.** ADG and EDG using measured *S*-parameter data.

Fig. 8. ECC using measured *S*-parameter data.

measured in an anechoic chamber. A broadband double ridged waveguide horn antenna operating between 1 and 12 GHz is used as a reference antenna to estimate the gain properties of the proposed antenna. The pattern diversity characteristics of the four-port MIMO antenna is evident through the radiation pattern plots showing pattern maxima in different directions. Thus, in the event of deep fading, at least one of the antennas will receive a better-quality signal leading to improved signal-to-noise ratio (SNR) performance. Thus, the proposed antennas increase the link reliability and also enhances the channel capacity. The realized gain of the antenna and the total efficiency of the four-port MIMO antenna is illustrated in Fig. 7. The measured peak gain of the antenna is greater than 5 dBi in all the ports and this peak occurs at 8 GHz. The mean of the gain offered by all the four ports is calculated and presented in Fig. 7. The authors could not measure the efficiency of the antenna due to resource limitation. The simulated efficiency of the antenna ranges between 73 and 86%.

Performance evaluation of MIMO metrics

The proposed four-port MIMO antenna is subjected to the evaluation of MIMO performance using some of the performance metrics such as ECC, apparent diversity gain (ADG), effective diversity gain (EDG) and mean effective gain (MEG).

ECC using S-parameters and far-field data

The ECC is a measure of the correlation between the radiation pattern of the individual antenna elements in the MIMO scheme.
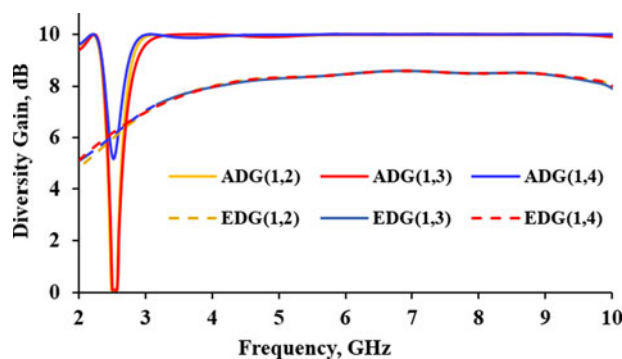
This parameter signifies the independent operation of the basic antenna elements. The ideal value of ECC is 0 and the acceptable level is 0.5. The more accurate form of ECC calculation is by using the far-field data. However, in places of resource limitations, the *S*-parameter-based equations can be used to estimate the ECC. The ECC using *S*-parameters and far-field data is given by equations (1) and (2), respectively. The ECC using measured *S*-parameters is shown in Fig. 8. From the figure, it is evident that the proposed antenna has a correlation coefficient <0.1 throughout the operating bandwidth. The simulated ECC using far-field data is found to be <0.4. During the calculation of far-field-based ECC, the cross-polarization ratio (XPR) is set be 1 dB relevant to the outdoor scenario. The power distribution is assumed to be Gaussian with mean and standard deviation set to 10° and 20°, respectively.

$$\text{ECC} = \frac{|S_{ii}^* S_{ij} + S_{ji}^* S_{jj}|^2}{(1 - |S_{ii}|^2 - |S_{ji}|^2)(1 - |S_{jj}|^2 - |S_{ij}|^2)} \quad (1)$$

$$\rho_e = \frac{|\iint \left(\vec{F}_i(\theta, \phi) \bullet \vec{F}_j(\theta, \phi)\right) d\Omega|^2}{\iint |\vec{F}_i(\theta, \phi)|^2 d\Omega \iint |\vec{F}_j(\theta, \phi)|^2 d\Omega} \quad (2)$$

Diversity gain using S-parameters and far-field data

The diversity gain (DG) is another useful metric in evaluating the MIMO performance of the proposed antenna. The ADG is the measure of the effective increase in the SNR after adopting the MIMO scheme. The theoretical limit for ADG is 10 dB. Another useful form of DG which takes into account the radiation losses from the antenna is the EDG. The ADG and EDG are calculated using (3) and (4) from the ECC values computed above. Under both circumstances, the ADG and EDG should be greater than 7.5 dB for an effective MIMO scheme. Figure 9 illustrates the ADG and EDG of the proposed four-port MIMO antenna using measured *S*-parameter data. From the figure, it is evident that the ADG is close to 10 dB and the EDG is greater than 7.5 dB throughout the operating bandwidth. The ADG and EDG using far-field data also satisfy the minimum requirement of the MIMO scheme. The ADG and EDG using far-field data are greater than 9 and 7 dB, respectively, under the settings described in the section "ECC using *S*-parameters and far-field data."

$$ADG = 10 \times \sqrt{1 - |ECC|^2} \quad (3)$$

Table 1. MEG ratio calculated with reference to port 1.

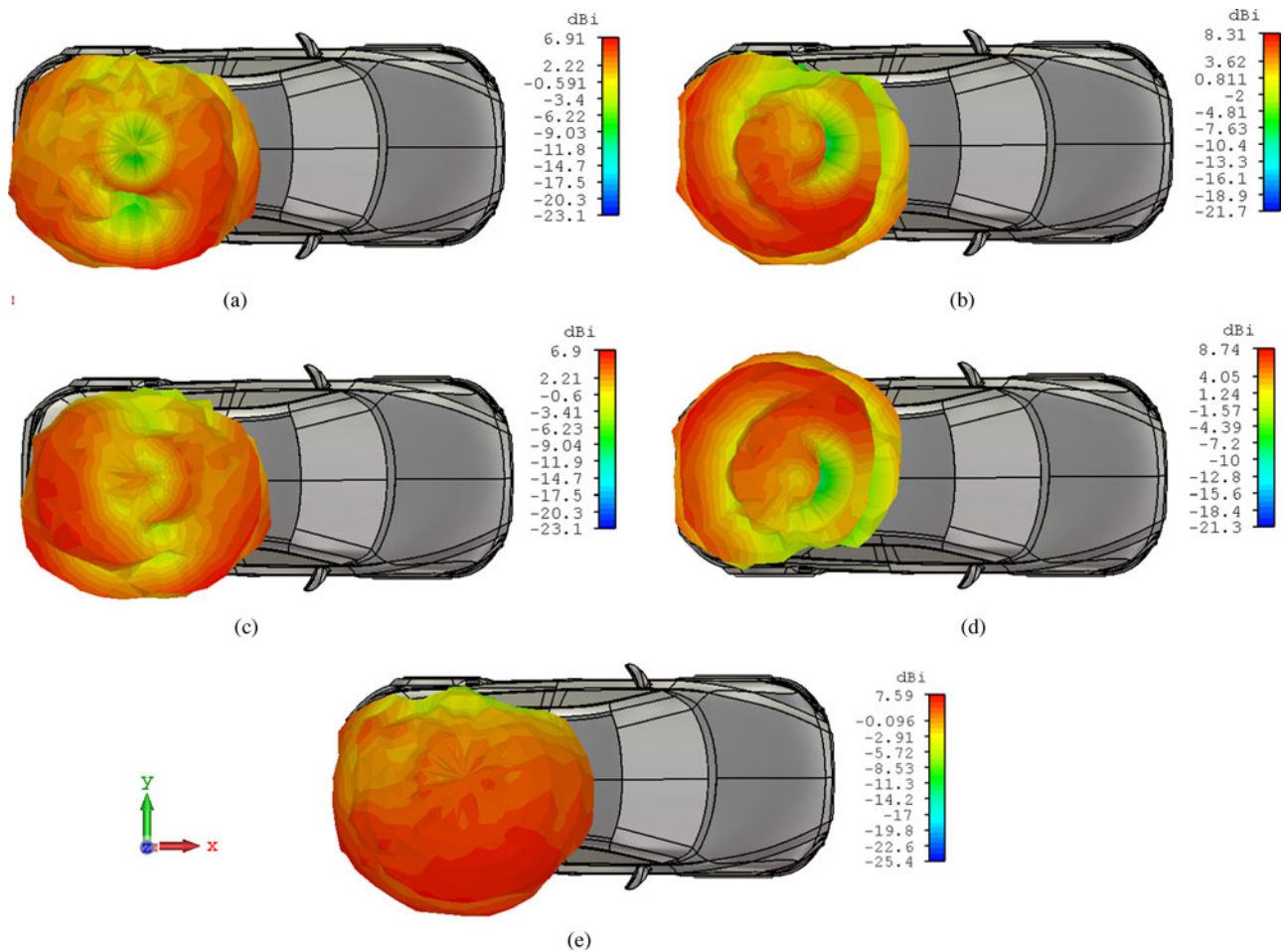| Sl. No.	Frequency (GHz)	Isotropic XPR = 0 dB			Outdoor XPR = 1 dB		
		$\frac{MEG1}{MEG2}$ (dB)	$\frac{MEG1}{MEG3}$ (dB)	$\frac{MEG1}{MEG4}$ (dB)	$\frac{MEG1}{MEG2}$ (dB)	$\frac{MEG1}{MEG3}$ (dB)	$\frac{MEG1}{MEG4}$ (dB)
1	4.0	−0.4	−0.4	−0.7	−1.1	−1.3	−1.5
2	5.0	−0.3	−0.4	−0.6	−1.0	−1.0	−1.6
3	6.0	−0.3	−0.4	−0.6	−1.2	−1.1	−1.7
4	7.0	−0.3	−0.4	−0.5	−1.1	−1.2	−1.6
5	8.0	−0.2	−0.4	−0.6	−1.1	−1.1	−1.5

Fig. 10. Simulated on car performance of the proposed MIMO antenna at 6 GHz calculated at (a) Port 1, (b) Port 2, (c) Port 3, (d) Port 4, (e) Combined radiation pattern.

$$EDG = \eta_{total} \times ADG = \eta_{total} \times 10 \times \sqrt{1 - |ECC|^2} \quad (4)$$

Mean effective gain

MEG is another useful parameter in the estimation of MIMO performance. Since identical antennas are used to construct the MIMO antenna, the gain offered by individual antenna elements should not deviate by a large number. The ideal theoretical limit

for MEG is 0 dB. However, a deviation by ±3 dB is permissible. The MEG is calculated using the gain pattern and power pattern of the antenna along both elevation plane and principal plane as given by equation (5). Table 1 describes the MEG ratio between the adjacent antennas in the MIMO antenna scheme. The calculation is made with reference to port 1. From the table, it is inferred that the deviation is within the acceptable level making the scheme more suitable for MIMO communications.

Table 2. Performance comparison with other four-port MIMO antennas.

Ref. No.	Size (mm³)	ϵ_r	No. of elements	Operating frequency (GHz)	Peak gain (dBi)	η%	Interport isolation (dB)
[4]	200 × 150 × 0.76	3.48	4	1.48–4.56	4.2	95	>15
[5]	50 × 35 × 1.0	4.3	2	3.0–11.0	>3	>80	>25
[6]	100 × 50 × 4.5	4.4	4	2.7–3.6	3.0	>80	>25
[7]	31 × 31 × 0.762	3.2	4	3.6–10. 6	NR	>52	>25
[8]	47 × 47 × 0.8	4.4	4	3.1–12	5.0	>70	>15
[9]	58 × 58 × 0.8	4.4	4	3.0–13.5	6.8	NR	>22
[10]	30 × 30 × 1.6	4.4	4	3.1–11	6.8	NR	>20
[11]	60 × 60 × 0.8	4.3	4	0.875–2.45	−1.50	NR	>16
[13]	120 × 65 × 1.6	4.4	4	3.3–5.0	4.71	NR	>18
[14]	145 × 75 × 0.8	4.4	8	3.5 & 5.0	NR	>35	NR
[15]	150 × 70 × 0.8	4.4	8	3.5 & 5.0	4.4 & 5.5	>61	>20
[16]	44 × 44 × 50	4.4	4	3.0–20.0	5.0	>80	>20
[21]	20 × 24 × 24	4.4	4	3.0–6.75	4.97	>80	>15
This work	32 × 15 × 32	2.5	4	2.8–9.50	5.41	>73	>15

$$MEG = \int_0^{2\pi}\int_0^{\pi} \left[\frac{XPR}{1+XPR}G_\theta(\theta,\phi)P_\theta(\theta,\phi) + \frac{1}{1+XPR}G_\phi(\theta,\phi)P_\phi(\theta,\phi) \right] \sin\theta d\theta d\phi \quad (5)$$

On-car performance evaluation

The on-car performance of the proposed MIMO antenna is evaluated using CST Microwave Studio. The radiation pattern of the individual antenna elements is used as a far-field source to evaluate the on-board characteristics. CST's asymptotic solver is used to estimate the on-car performance of the proposed antenna. The asymptotic solver is used to calculate the fields radiated by an antenna in the presence of large electrical structures. The asymptotic solver efficiently computes the scattered fields using 3D ray tracing method. The 3D CAD model of Toyota's Mazda is used for the calculation of the far-field properties. Antennas for automotive applications should satisfy certain important requirements to achieve high performance. For instance, the antenna should be placed high above the ground to avoid ground reflections. The car's roof is an ideal location for loading the antenna in automobiles. In this region, the antenna sees no metallic obstructions except the car roof. Therefore, the proposed MIMO antenna is mounted at the rear end of the roof where the shark fin housing is loaded. The shark fin has a typical dimension of 179 mm × 88 mm × 55 mm which can easily accommodate the proposed four-port antenna whose footprint is 32 mm × 15 mm × 32 mm. The antenna is positioned 1 cm above the car's roof. The 1 cm gap between the vehicle's roof and the antenna base corresponds to the base of the shark-fin housing [19]. In the simulation, the effect of housing neglected and hence the surrounding environment is assumed to be free space. Figure 10 illustrates the simulated on-car performance of the proposed MIMO antenna at 6 GHz. Furthermore, Figs 10(a)–10(d) correspond to the radiation pattern of antenna elements 1–4,

respectively. From the figure, it can be inferred that the radiation patterns are unique for each antenna element. The nulls present in some antenna elements are compensated by maximum gain offered by other antenna elements. To understand the overall radiation performance, the combined radiation pattern is plotted in Fig. 10(e). From Fig. 10(e), it can be seen that the proposed MIMO antenna provides a maximum gain in all directions. Furthermore, the directivity of the proposed MIMO antenna shows at least 3 dB increment since the roof is assumed to be a conductor which diffracts the backward radiation. This phenomenon has been extensively studied in [1, 20]. The diffraction effect increases the overall realized gain of the proposed antenna. Since the antenna is loaded in the car's roof, the other parts of the vehicle body have negligible influence on the antenna's radiation characteristics.

Thus, the operation of the antenna in the presence of the scattering environment is validated making the antenna suitable for real-time application. Table 2 compares the performance of the proposed antenna with the state-of-the-art reported in the literature. The proposed antenna is a 3D solution with vertical polarization unlike many other antennas [1–15] reported in the literature. The antenna is constructed using common ground configuration unlike [7–9, 17, 18]. Most of the MIMO antennas [12–15] are reported for smartphone applications. However, the proposed antenna is more suitable for the vehicular environment. The 3D antenna in [16] occupies more space than the proposed antenna. Though the antenna in [21] is smaller than the proposed antenna, the bandwidth is limited to 3.75 GHz.

Conclusion

The design of a four-port MIMO antenna with the interlocked scheme is presented for UWB applications in the automotive environment. The proposed MIMO antenna has a compact geometry and hence it is suitable for roof-top loading primarily inside the shark fin housing. The S-parameter and radiation characteristics of the four-element MIMO are simulated using CST

Microwave Studio and the simulation results are verified using experimental measurements. The MIMO parameters such as ECC, ADG, EDG, and MEG are evaluated and presented. The realized DG in close to 10 dB making the antenna suitable for MIMO communications. The influence of the vehicle's body on the radiation characteristics is evaluated and the results are presented. From the on-car performance evaluation results, it is inferred that the proposed four-element MIMO antenna has high gain and omnidirectional coverage improving the wireless link reliability.

References

1. **Zhao X, Yeo SP and Ong LC** (2018) Planar UWB MIMO antenna with pattern diversity and isolation improvement for mobile platform based on the theory of characteristic modes. *IEEE Transactions on Antennas and Propagation* **66**, 420–425.
2. **Roshna TK, Deepak U, Sajitha VR, Vasudevan K and Mohanan P** (2015) A compact UWB MIMO antenna with reflector to enhance isolation. *IEEE Transactions on Antennas and Propagation* **63**, 1873–1877.
3. **Nie LY, Lin XQ, Yang ZQ, Zhang J and Wang B** (2019) Structure-shared planar UWB MIMO antenna with high isolation for mobile platform. *IEEE Transactions on Antennas and Propagation* **67**, 2735–2738.
4. **Hussain R and Sharawi MS** (2019) An integrated slot-based frequency-agile and UWB multifunction MIMO antenna system. *IEEE Antennas and Wireless Propagation Letters* **18**, 2150–2154.
5. **Wang L, Du Z, Yang H, Ma R, Zhao Y, Cui X and Xi X** (2019) Compact UWB MIMO antenna with high isolation using fence-type decoupling structure. *IEEE Antennas and Wireless Propagation Letters* **18**, 1641–1645.
6. **Chattha HT** (2019) 4-Port 2-Element MIMO antenna for 5G portable applications. *IEEE Access* **7**, 96516–96520.
7. **Sipal D, Abegaonkar MP and Koul SK** (2018) Compact planar 2×2 and 4×4 UWB MIMO antenna arrays for portable wireless devices. *Microwave and Optical Technology Letters* **60**, 86–92.
8. **Mathur R and Dwari S** (2018) Compact CPW-fed ultrawideband MIMO antenna using hexagonal ring monopole antenna elements. *AEU – International Journal of Electronics and Communications* **93**, 1–6.
9. **Raheja DK, Kanaujia BK and Kumar S** (2019) Compact four-port MIMO antenna on slotted-edge substrate with dual-band rejection characteristics. *International Journal of RF and Microwave Computer-Aided Engineering* **29**, e21756.
10. **Prabhu P and Malarvizhi S** (2019) Novel double-side EBG based mutual coupling reduction for compact quad port UWB MIMO antenna. *AEU – International Journal of Electronics and Communications* **109**, 146–156.
11. **Kumar A, Ansari A, Kanaujia B and Kishor J** (2018) High isolation compact four-port MIMO antenna loaded with CSRR for multiband applications. *Frequenz* **72**, 415–427.
12. **Liu Y, Lu Y, Zhang Y and Gong S** (2019) "MIMO Antenna array for 5G smartphone applications," *2019 13th European Conference on Antennas and Propagation (EuCAP)*, Krakow, Poland, 2019, pp. 1–3.
13. **Biswas A and Gupta VR** (2020) Design and development of low profile MIMO antenna for 5G new radio smartphone applications. *Wireless Personal Communications* **111**, 1695–1706.
14. **Yan K, Yang P, Yang F, Zeng LY and Huang S** (2018) "Eight-antenna array in the 5G smartphone for the dual-band MIMO system," *2018 IEEE International Symposium on Antennas and Propagation & USNC/URSI National Radio Science Meeting*, Boston, MA, 2018, pp. 41–42.
15. **Wei G and Feng Q** (2020.) Dual-band MIMO antenna array for compact 5G smartphones. *Progress in Electromagnetics Research C* **99**, 157–165.
16. **Srivastava K, Kanaujia BK, Dwari S, Kumar S and Khan T** (2019) 3D cuboidal design MIMO/diversity antenna with band notched characteristics. *AEU – International Journal of Electronics and Communications* **108**, 141–147.
17. **Premalatha J and Sheela D** (2020) Compact four-port vertically polarized UWB monopole antenna for MIMO communications. *Circuit World*. doi: 10.1108/CW-04-2020-0055.
18. **Reddy GS, Kamma A, Kharche S, Mukherjee J and Mishra SK** (2015) Cross-configured directional UWB antennas for multidirectional pattern diversity characteristics. *IEEE Transactions on Antennas and Propagation* **63**, 853–858.
19. **Chakam GA, Schürmeier M, Butscher F and Mierke F** (2012) 'Highly integrated multiband shark fin antenna for a vehicle', US 20120274519 A1.
20. **Naga Sai GP, Suneel Kumar K, Sunil Kumar SM and Kandimalla D** (2018) "Quarter wavelength monopole antenna on flat conducting plates: uniform theory of diffraction," *2018 IEEE Indian Conference on Antennas and Propagation (InCAP)*, Hyderabad, India, 2018, pp. 1–4.
21. **Bactavatchalame P and Rajakani K** (2020) Compact broadband slot-based MIMO antenna array for vehicular environment. *Microwave and Optical Technology Letters* **62**, 2024–2032.

M. Saravanan received his B.E. degree in Electronics and Communication Engineering and M.E. degree in Communication Systems from Anna University, Chennai in 2006 and 2009, respectively. He is currently an Assistant Professor in the Department of Electronics and Communication Engineering at Anand Institute of Higher Technology, Chennai. His research interest includes Distributed Systems, Spectrum Sharing, Antenna Engineering, and Cognitive Radio systems.

Dr. R. Kalidoss completed bachelor's degree (B.E., 2004) in Electronics and Communication Engineering from Madurai Kamaraj University and master's degree (M.E., 2006) in Communication Systems from Anna University, Chennai. Further, he obtained a doctoral degree (Ph.D., 2015) from Anna University, Chennai. He currently holds an academic post as an Associate Professor in the Department of ECE, Sri Siva Subramaniya Nadar College of Engineering, Chennai. His current research interests include Adaptive Channel Modeling in Cognitive Radio, Advanced Spectrum Utilization, and Cognitive Radio Architecture. He has published/presented over 30 research articles in refereed International/National Journals/Conferences.

Dr. B. Partibane received his B.E. degree in ECE from Madras University, Chennai, in 1999, and the M.Tech degree in ECE from Pondicherry University, Pondicherry, in 2003. Further, he obtained a doctoral degree from Anna University, Chennai in 2017. He currently holds an academic post as Associate Professor in the Department of ECE, SSN Institutions. He is an author and co-author of research publications in National / International Conferences and International Journals. His research interests include Wireless Communication and Networks, Antenna Engineering and Security in Ad hoc and Sensor Network.

Dr. K.S.Vishvaksenan received an M.S. (system software) degree from Birla Institute of Technology and Science, Pilani, Rajasthan, India in 1997, and M.E. degree from College of Engineering, Guindy, Anna University, Chennai, India in 2007. He has been awarded Ph.D. degree from the College of Engineering, Guindy, Anna University, Chennai, India in the year 2013. He is working in SSN Institutions as an Associate Professor in the Department of ECE. He has authored or co-authored 30 IEEE International Conferences and 36 International Journals. His research field includes the MIMO Detection Algorithm, Iterative Receiver Algorithm, Multi-user Communications, Co-operative Communication, Cognitive Radio Network, and Transmitter Pre-processing Techniques.